American Journal of Pathology, Vol. 164, No. 2, February 2004

Retinal Dystrophy Resulting from Ablation of RXRα in the Mouse Retinal Pigment Epithelium

Mikiro Mori,*† Daniel Metzger,* Serge Picaud,† Colette Hindelang,* Manuel Simonutti,† José Sahel,† Pierre Chambon,*‡ and Manuel Mark*‡

From the Institut de Génétique et de Biologie Moléculaire et Cellulaire and the Laboratoire de Physiopathologie Cellulaire et Moléculaire de la Rétine,† Centre National de la Recherche Scientifique, Institut National de la Santé et de la Recherche Médicale, Université Louis Pasteur, Collège de France, Strasbourg; and the Institut Clinique de la Souris,‡ Strasbourg, France*

Vitamin A (retinol) actions in eye development are mediated by retinoic acid receptors (RARs and RXRs). Using the Cre/loxP system, we have selectively ablated RXRα in the retinal pigment epithelium (RPE), a cell monolayer critically involved in visual retinoid renewal and phagocytosis of photoreceptor outer segments. In the mutant (RXRα $^{rpe-/-}$) mice, RPE cells are morphologically and functionally abnormal and display decreased expression of proteins involved in the visual retinoid cycle, namely RPE65, CRALBP, and RGR. RXRα $^{rpe-/-}$ mice also show alterations of photoreceptor cells including: 1) decrease in their number; 2) outer segment shortening and disorganization, and 3) reduced light responses in electroretinograms. These results indicate that RXRα is required for normal maturation of the RPE, which is known to play essential roles in photoreceptor cell function and survival, and point to a possible involvement of RXRα signaling pathways in the RPE in human retinal diseases. ***(Am J Pathol 2004, 164:701–710)***

The functions of vitamin A (retinol) in eye development are mediated by its active derivative, retinoic acid (RA).[1,2] RA activates two families of nuclear receptors, the retinoic acid receptors, RARs (α, β, and γ), and the retinoid X receptors, RXRs (α, β, and γ), which are ligand-dependent transcriptional regulators.[3] RXRα plays major roles in eye development as demonstrated by the multiple ocular abnormalities displayed by RXRα-null mutant fetuses,[4] but the death of these mutant fetuses around E14.5 has precluded the establishment of RXRα functions at later stages of eye development and in adulthood.

In the adult eye, vitamin A is critically involved in vision as a source of *11-cis*-retinaldehyde, the chromophore of opsins in mammalian photoreceptors.[5,6] Regeneration of this chromophore as well as phagocytoses of distal portions of the continuously growing photoreceptor outer segments is performed by the retinal pigment epithelium (RPE), a cell monolayer lying between the choroid and the photoreceptor cells.[7,8] The requirement of RPE in eye development and in retinal function and survival has been demonstrated by RPE ablation experiments using RPE-specific expression of the diphtheria toxin in transgenic mice,[9] as well as by the occurrence of retinal dystrophies in rodents or humans carrying mutations in genes expressed in the RPE (eg, *RPE65*,[10–13] *RGR*,[14,15] and *RLBP1*[16,17]). RPE dysfunction is also involved in the pathogenesis of age-related macular degeneration, which is the major and increasing cause of vision loss among the elderly of the industrialized world.[18,19]

To investigate the roles of RXRα in the RPE, we have generated mutant mice in which RXRα is selectively inactivated in this tissue, using a tyrosinase-related protein 1 (TRP1) promoter-driven Cre recombinase.[20–22] We found that these mice exhibit dystrophic changes in the RPE and retina accompanied by photoreceptor dysfunction. This mouse phenotype indicates that RXRα present in the RPE is required both for RPE development and for neural retina maintenance, and points to a possible involvement of RXRα signaling pathways in the RPE in human retinal diseases.

Materials and Methods

Transgenic Mice

RXRα $^{L2/+}$ mice, in which the exon encoding the DNA binding domain of RXRα is loxP-flanked (floxed) on one allele,[23] were bred with TRP1-Cre $^{(tg/0)}$ transgenic mice that express the Cre recombinase under the control of

Supported by grants from the Centre National de la Recherche Scientifique; the Institut National de la Santé et de la Recherche Médicale (to M.M.); the Collège de France; the Institut Universitaire de France; the Hôpital Universitaire de Strasbourg; the Association pour la Recherche sur le Cancer; the Fondation pour la Recherche Médicale; the Ministry of Education, Culture, Sports, Science, and Technology of Japan (to M. M.); and the Foundation Fighting Blindness (to M. M.).

Accepted for publication October 9, 2003.

Present address of M. M.: Department of Ophthalmology, Jichi Medical School, Minamikawachi, Tochigi 329-0498, Japan.

Address reprint requests to Pierre Chambon, Institut Clinique de la Souris (ICS), BP 10142, 67404 Illkirch Cedex, C.U de Strasbourg, France. E-mail: chambon@igbmc.u-strasbg.fr.

TRP1. The patterns of Cre expression and DNA excision in this mouse line have been reported previously.[22] All mice harboring the TRP1-Cre transgene were genotyped for *rd* (retinal degeneration) mutation[24] that was present in the founder mouse of FVB/N background,[25] and mice that did not carry the *rd* mutation were used. Mice were maintained on a 12-hour light/dark cycle with food and water provided *ad libitum*.

Electroretinogram (ERG)

Six-month-old mice were dark-adapted for at least 16 hours and anesthetized by intraperitoneal injection of ketamine (200 mg/kg body weight) and xylazine (10 mg/kg body weight). Pupils were dilated by topical application of 1% atropine sulfate. Full-field ERGs were recorded in a Ganzfeld dome using a gold-coil active electrode on the corneal surface, a subcutaneous reference electrode on the head between the eyes, and a needle ground electrode on the tail. Methylcellulose was applied between the cornea and the electrode speculum for their tight connection.

Scotopic ERG responses were recorded with single flash stimuli ranging from 10^{-4} cd s/m^2 to 25 cd s/m^2. Responses were recorded once with a flash of a given intensity, because response tended to decrease when recorded repeatedly. Photopic ERG responses were recorded after 10 minutes of exposure to background light of 30 cd/m^2. Single flash responses were obtained with 1, 10, and 25 cd s/m^2. Flicker responses were obtained with flashes of 3 cd s/m^2 at frequencies ranging from 0.5 to 30 Hz.

For recovery experiments, mice were dark-adapted at least for 16 hours and anesthetized as described above. Maximal scotopic responses were recorded using a 0.1 cd s/m^2 stimulus. Bleaching was done in a Ganzfeld dome with 0.2 cd/m^2 illumination for 5 minutes. Throughout a 25-minute period, single responses were recorded every 5 minutes using a single 0.1 cd s/m^2 stimulus.

Histology and Electron Microcopy

Eyes were removed 4 hours after the onset of light (11:00), immersion-fixed in either Bouin's fluid or in 2.5% glutaraldehyde in phosphate-buffered saline (PBS), and processed as described.[26] Briefly, the Bouin-fixed eyes were bisected along the vertical meridian, embedded in paraffin, sectioned at 5 μm, and stained with hematoxylin and eosin. Glutaraldehyde-fixed eyes were bisected and embedded in epon. One-μm-thick sections were stained with toluidine blue for light microscopy, and 90-nm-thick sections were contrasted with uranyl acetate and lead citrate for electron microscopy. Outer segment lengths were measured at a distance of 1.0 mm from the optic nerve head on 1-μm-thick sections from five animals. The numbers of nuclear rows in the outer nuclear layer were calculated as mean values of three counts in the same region. To evaluate the numbers of phagosomes in the RPE, all densely stained inclusions larger than 0.75 μm in any dimensions and contained in the cell soma or villous processes were counted along the entire, 1-μm-thick, eye sections from 3-month-old mice as described.[27]

Immunohistochemistry

For RXRα immunodetection, albino embryos, which do not have melanin granules in the RPE, were collected at embryonic day 13.5 (E13.5) and immersion-fixed in a poly-L-lysine-paraformaldehyde fixative. Ten-μm-thick frontal cryosections at the level of the optic nerve head were processed for fluorescent immunolabeling with a polyclonal anti-RXRα antibody as described.[28] For immunodetection of vision-related proteins (CRALBP, RGR, RPE65, arrestin, rhodopsin, cone red/green pigment, and cone blue pigment), heads from E17.5 fetuses as well as eyes from P4, P12, and 6-month-old mice were immersion-fixed in 4% paraformaldehyde in PBS at 4°C for 16 hours and embedded in paraffin. Three-μm sections were deparaffinized, treated with 0.25% $KMnO_4$ for 20 minutes and then with 5% oxalic acid for 3 minutes to bleach melanin granules, and immunolabeled with primary antibodies in PBS containing 5% normal goat serum at 4°C for 16 hours. The antibodies (all given to us as gifts) were: anti-CRALBP (rabbit polyclonal, 1:1000), anti-RGR (rabbit polyclonal, 1:200), anti-RPE65 (mouse monoclonal, 1:1000), anti-arrestin (rabbit polyclonal, 1:5000), anti-rhodopsin (mouse monoclonal, 4D2; 1:5000), anti-red/green cone pigment and anti-blue cone pigment (both rabbit polyclonal, 1:5000). The secondary antibodies were labeled with Alexa 488 or Alexa 594 (1:500; Molecular Probes, Eugene, OR). All immunolabelings were photographed in the central regions of the retina/RPE near the optic nerve head, unless otherwise specified.

Reverse Transcriptase (RT)-Polymerase Chain Reaction (PCR)

Eyes of 6-month-old mice were dissected and eyecups consisting of the RPE, choroid, and sclera were isolated. Total RNA was extracted from two eyecups of one animal using a kit (EasyPrep; Takara, Tokyo, Japan) according to the manufacturer's instructions. One μg of RNA was treated with DNaseI (Takara), and first-strand cDNA was synthesized using a kit with an oligo-dT primer (Roche, Indianapolis, IN) according to the manufacturer's instructions. PCR was performed to amplify DNA segments of RPE65, CRALBP, RGR, and a housekeeping gene, glyceraldehyde-3-phosphate dehydrogenase (G3PDH) using 0.5 μmol/L of primers at 94°C, 58°C, and 72°C (30 seconds each). The primers used were as follows: RPE65, 5′-AATGGATTTCTGATTGTGGA-3′ and 5′-TCAGGATCTTTTGAACAGTC-3′; CRALBP, 5′-CAAGAGGCAGTATGTCAGAC-3′ and 5′-GAAGAGTTCAGGGTACTGGA-3′; RGR, 5′-TGACCATCTTCTCTTTCTGC-3′ and 5′-GGGTGCAGTAGTGGTGATAA-3′; G3PDH, 5′-GCATCCTGGGCTACACTGAG-3′ and 5′-TTTACTCCTTGGAGGCCATG-3′.

For semiquantitative evaluation, 24, 27, and 30 PCR cycles were performed for CRALBP, RPE65, and RGR,

and 18, 21, and 24 cycles for G3PDH. The PCR products were electrophoresed on a 2.5% agarose gel, stained with ethidium bromide, and photographed under ultraviolet light. The density of the bands was quantified with an optical scanner and standardized with that of G3PDH after 21 PCR cycles (exponential amplification phase). The nucleotide sequences of the products were confirmed with an automated DNA sequencer.

TdT-Mediated UTP Nick-End Labeling (TUNEL) Analysis

Histological sections from 4% paraformaldehyde-fixed, paraffin-embedded, eyes from 3-month-old mice were processed for TUNEL analysis (Apoptosis Detection System; Promega, Madison, WI) according to the manufacturer's instructions and observed under a fluorescent microscope.

Statistical Analyses

Data from mutant and control mice were compared using the unpaired two-tailed Student's *t*-test with Welch correction for unequal variance.

Results

Efficient Ablation of RXRα in the RPE of RXRα $^{rpe-/-}$ Mice

To ablate RXRα in the RPE, RXRα $^{L2/+}$ mice were bred with TRP1-Cre $^{(tg/0)}$ transgenic mice to generate TRP1-Cre $^{(tg/0)}$/RXRα $^{L2/L2}$ mice (referred to as RXRα $^{rpe-/-}$ mice hereafter). TRP1-Cre $^{(tg/0)}$/RXRα $^{+/+}$, TRP1-Cre $^{(0/0)}$/RXRα $^{+/+}$, and TRP1-Cre $^{(0/0)}$/RXRα $^{L2/L2}$ littermates, all of which displayed no morphological eye abnormalities, served as controls. At embryonic day (E) 13.5, RXRα protein was detected both in the periocular mesenchyme (PM) and RPE of control mice (Figure 1a, arrows), while it was selectively absent in the RPE of the RXRα $^{rpe-/-}$ mouse (Figure 1b, arrows). Weak immunostaining in the neural retina (N), which was not visible at the low magnification in Figure 1, a and b, was similar in control and RXRα $^{rpe-/-}$ mice. These results indicate that RXRα is selectively and efficiently depleted in the RPE of RXRα $^{rpe-/-}$ fetuses.

Reduced ERG Response and Delayed Dark Adaptation in RXRα $^{rpe-/-}$ Mice

ERGs were performed in 6-month-old mice to study the function of RPE and photoreceptor cells. To assess the function of the rod pathway, scotopic responses were recorded at different light intensities. Both a- and b-wave amplitudes were reduced by ~50% in RXRα $^{rpe-/-}$ mice as compared with control mice (Figure 2; a to d). To assess the function of the cone pathway, flicker and photopic responses were recorded. The b-wave amplitudes in both flicker and photopic ERGs were similarly reduced by ~50% as compared with control mice (Figure 2, e and f). In contrast, there were no significant differences between RXRα $^{rpe-/-}$ and control mice in the latency for the a- and b-waves in scotopic ERGs, as well as in the b-waves in flicker and photopic ERGs (data not shown).

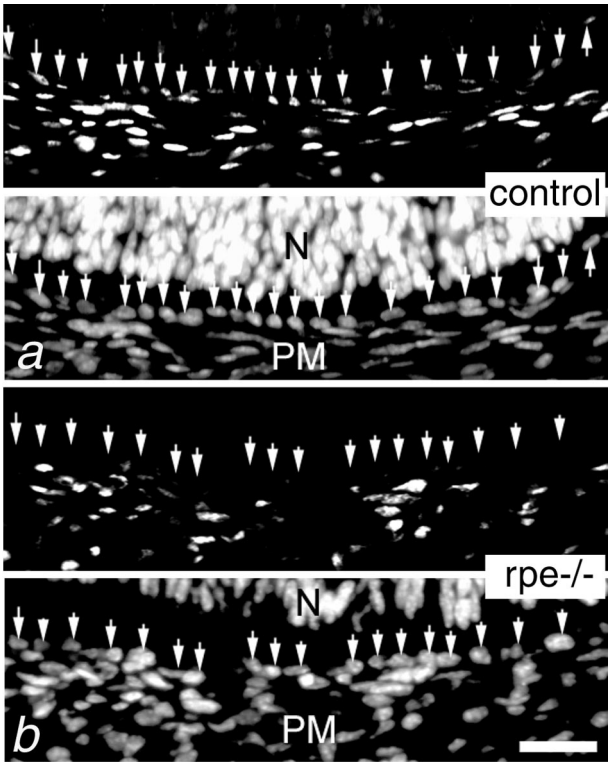

Figure 1. Selective ablation of RXRα in the RPE. Immunodetection of RXRα in the E13.5 control (**a**) and RXRα $^{rpe-/-}$ (rpe−/−, **b**) eyes. The **top** half of each panel corresponds to the immunohistochemical signal and the **bottom** half to the DAPI counterstaining. **Arrows** point to RPE cell nuclei. N, neural retina; PM, periocular mesenchyme. Scale bar, 10 μm.

As RPE cells are involved in visual retinoid renewal, their function was assessed by ERG before and after photo-bleach. After a 16-hour dark adaptation, scotopic responses were recorded with a single flash. This measurement confirmed that a-wave amplitudes were reduced by ~50% in RXRα $^{rpe-/-}$ mice as compared with control mice (Figure 3). Subsequently, after a 10-minute photo-bleach, scotopic responses were recorded at 5-minute intervals with the same flash intensity as in the prebleach measurement. Control mice recovered ~40% of their prebleach a-wave amplitudes within 25 minutes, whereas RXRα $^{rpe-/-}$ mice exhibited a low recovery (<10%) (Figure 3), indicating impairment of visual retinoid renewal.

Dystrophic Changes of RPE in RXRα $^{rpe-/-}$ Mice

Histological analysis of the RXRα $^{rpe-/-}$ mice revealed no abnormalities at E17.5 and postnatal day 4 (P4) (data not shown). In contrast, the mutant RPE at P12 was thinner than control RPE and displayed an uneven distribution of

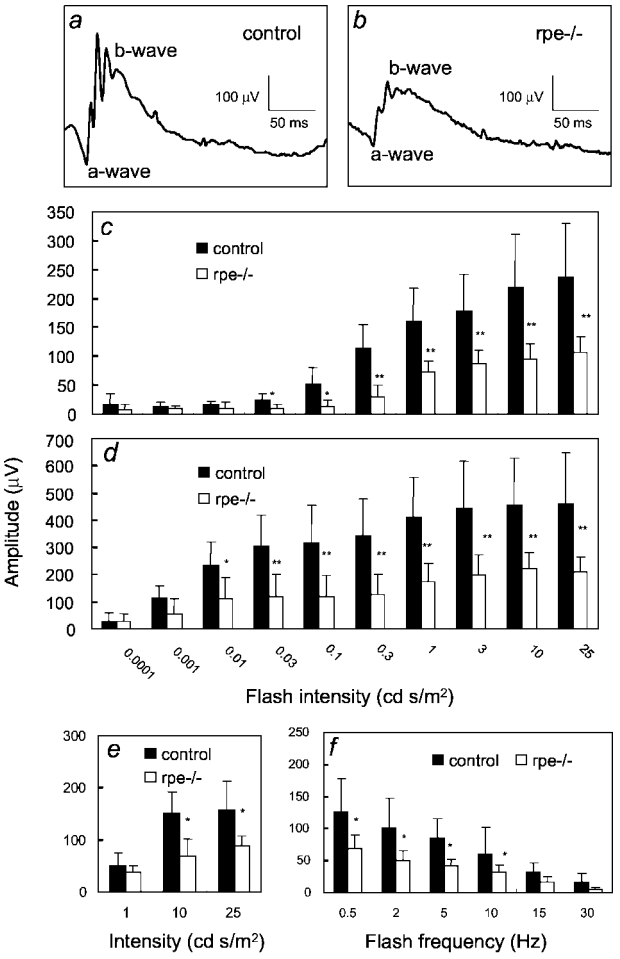

Figure 2. ERG analyses. Representative scotopic responses in a control (**a**) and RXRα $^{rpe-/-}$ (rpe−/−, **b**) mouse by 0.1 cd s/m^2 flash. Amplitudes of both a-waves (**c**) and b-waves (**d**) of scotopic ERGs, as well as of b-waves of photopic (**e**) and flicker (**f**) ERGs are reduced in the RXRα $^{rpe-/-}$ mice. Mean ± SD; *, $P < 0.05$; **, $P < 0.005$ ($n = 6$, *t*-test).

melanin granules (data not shown). In 3-, 12-, and 18-month-old RXRα $^{rpe-/-}$ mice, the thickness of the entire RPE was decreased (Figure 4, a to h, and data not shown). The mutant RPE cells contained fewer melanin granules than their counterpart in control mice (MG; Figure 4, compare c and d and g and h) and often displayed large vacuoles (V, Figure 4h). Large cysts (CY) and ectopic RPE cells (E) were frequently observed in the photoreceptor outer segment layer of the RXRα $^{rpe-/-}$ retina (Figure 4d, and see below). The number of phagosomes per mm of RPE was 29.4 ± 3.3 and 15.6 ± 2.6 (mean ± SD) in the 3-month-old control and RXRα $^{rpe-/-}$ mutant mice, respectively, and this difference was statistically significant ($P < 0.01$; *t*-test, $n = 5$). The RPE of 3-, 12-, and 18 month-old TRP1-Cre $^{(tg/0)}$/RXRα $^{L2/+}$ mice (ie, RXRα $^{rpe+/-}$mice) was histologically indistinguishable from that of control mice (data not shown).

Electron microscopy analysis showed that RPE cells of the 3-month-old RXRα $^{rpe-/-}$ mice were abnormally flat and elongated, and often largely overlapped with one another (eg, C1 and C2; Figure 5a). Control RPE cells never overlapped and were connected by tight junctions (Figure 5c, double arrow). In the areas of overlapping, RPE cells displayed loose intercellular contacts (Figure 5a, black arrows). Additionally, in mutant RPE cells, apical microvilli (MV) were shorter, extended less deeply into the interphotoreceptor space, contained fewer melanin granules (MG; Figure 5, compare a and b), and basal membrane infoldings (BI), which were well organized, lying parallel to one another in control RPE (Figure 5, b and c), were either absent or scarce (Figure 5; a, d, and e) and oriented randomly (Figure 5, f and g). The shape of the melanin granules was irregular, and typical fusiform granules were almost lacking (MG; Figure 5, compare a and b). Cells containing melanin granules observed between the photoreceptor outer segments of the RXRα $^{rpe-/-}$ retina most probably correspond to ectopic RPE cells (E, Figure 5a). Vacuoles (V, Figure 5a), electron-dense large phagolysosomes (P; Figure 5, d and f), and lipid droplets (LI, Figure 5e) were often found in RXRα $^{rpe-/-}$ mice but rarely or never in control mice. These observations indicate that some of the structural defects of the mutant RPE cells might be related to a metabolic disorder. Extracellular basal deposits of amorphous material, thickening of the Bruch's membrane (BM), and atrophy of the choroid (CH) were absent (Figure 5, a to e, and data not shown).

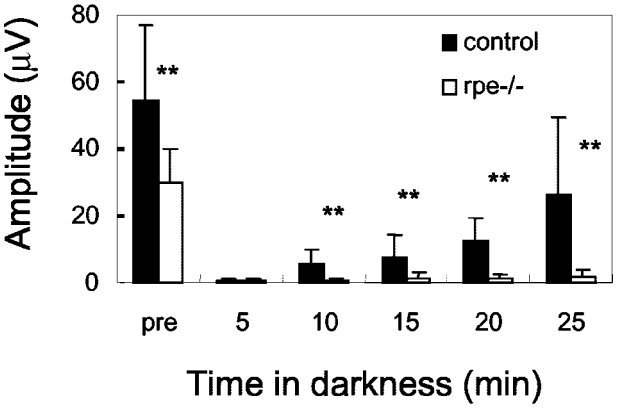

Figure 3. Dark adaptation analysis. After light bleach (0.2 cd/m^2 for 5 minutes), RXRα $^{rpe-/-}$ mice (rpe−/−) show little recovery of ERG a-wave amplitudes in 25 minutes, whereas the recovery in the control mice is ~40%. Mean ± SD; *, $P < 0.05$; **, $P < 0.005$ ($n = 6$, *t*-test).

Disorganization and Shortening of Photoreceptor Outer Segments and Decrease in the Number of Photoreceptor Cells in RXRα $^{rpe-/-}$ Mice

In RXRα $^{rpe-/-}$ mice, the photoreceptor cells appeared histologically normal at P12, ie, a time when their morphological differentiation is completed (data not shown). However, from 1 month of age onwards, photoreceptor outer segments no longer displayed the regular alignment seen in controls (OS; Figure 4, c, d, g, and h, and data not shown) and were significantly shorter (77%, 66%, and 65% of control at 3, 12, and 18 months, respectively; Figure 4, a to i). In contrast, inner segments had a normal size (IS; Figure 4, a to h). The number of

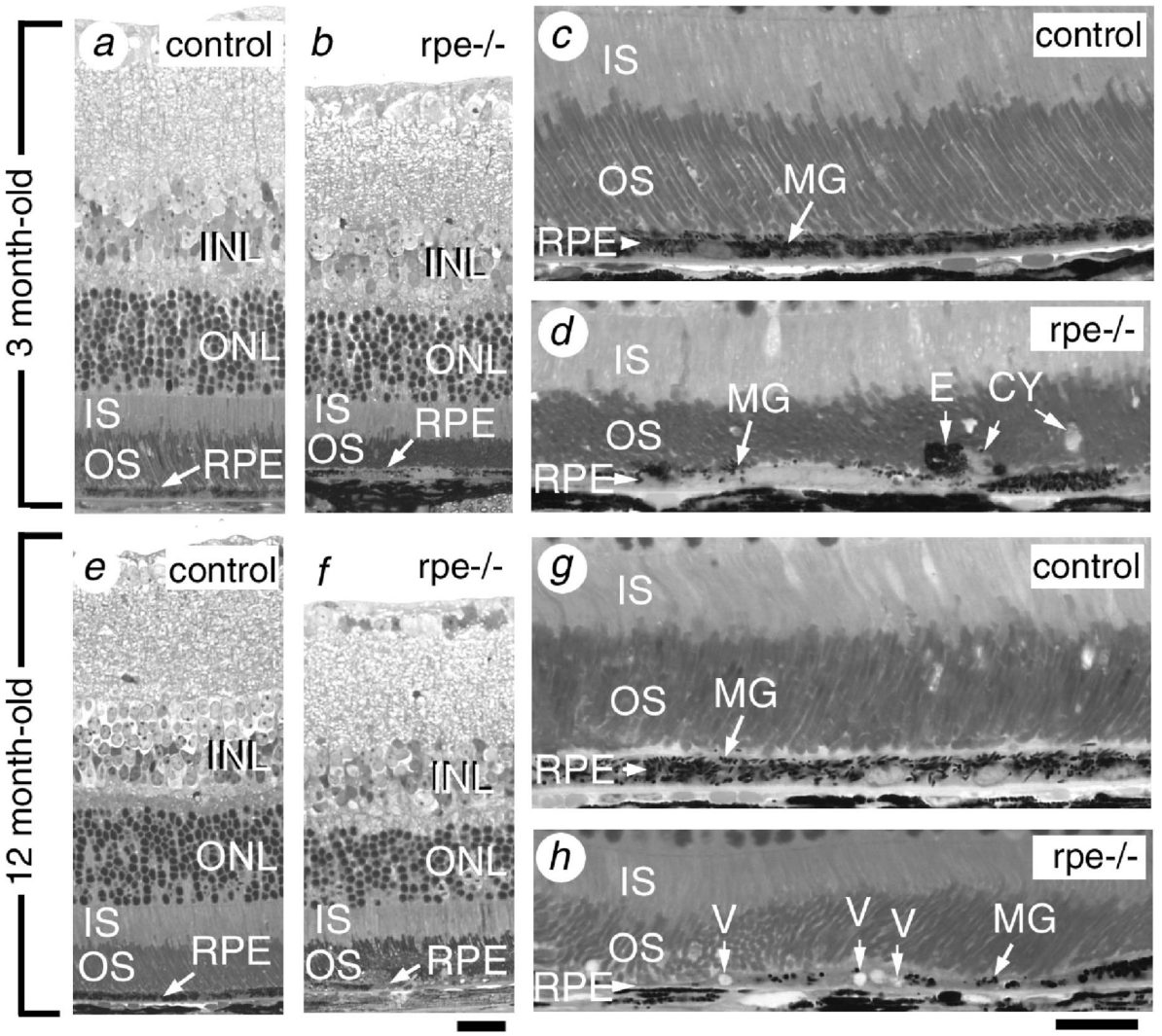

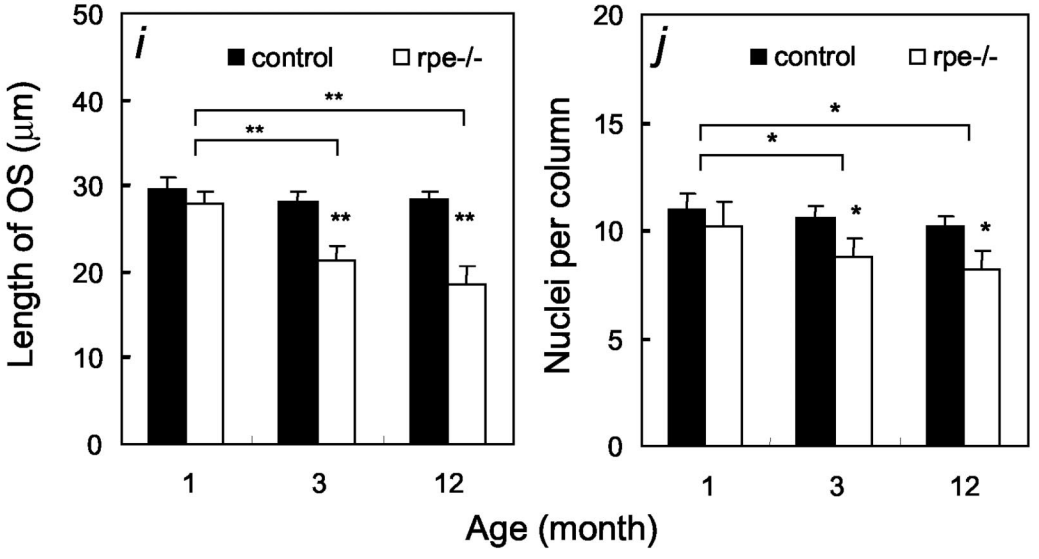

Figure 4. Histological abnormalities in RPE and neural retina of adult RXRα $^{rpe-/-}$ mice. Semithin sections through the retina of 3-month-old (**a–d**) and 12-month-old (**e–h**) control (**a**, **c**, **e**, and **g**) and RXRα $^{rpe-/-}$ (rpe−/−; **b**, **d**, **f**, and **h**) mice. **i** and **j:** Reduction of outer segment length (**i**) and of number of nuclear rows in the outer nuclear layer (**j**) of RXRα $^{rpe-/-}$ mice. Mean ± SD; *, $P < 0.05$; **, $P < 0.005$ ($n = 5$, *t*-test). CY, cysts; E, ectopic RPE cell; INL, inner nuclear layer; IS, photoreceptor inner segment; MG, melanin granules; ONL, outer nuclear layer; OS, photoreceptor outer segment; V, vacuoles. Scale bars, 20 μm.

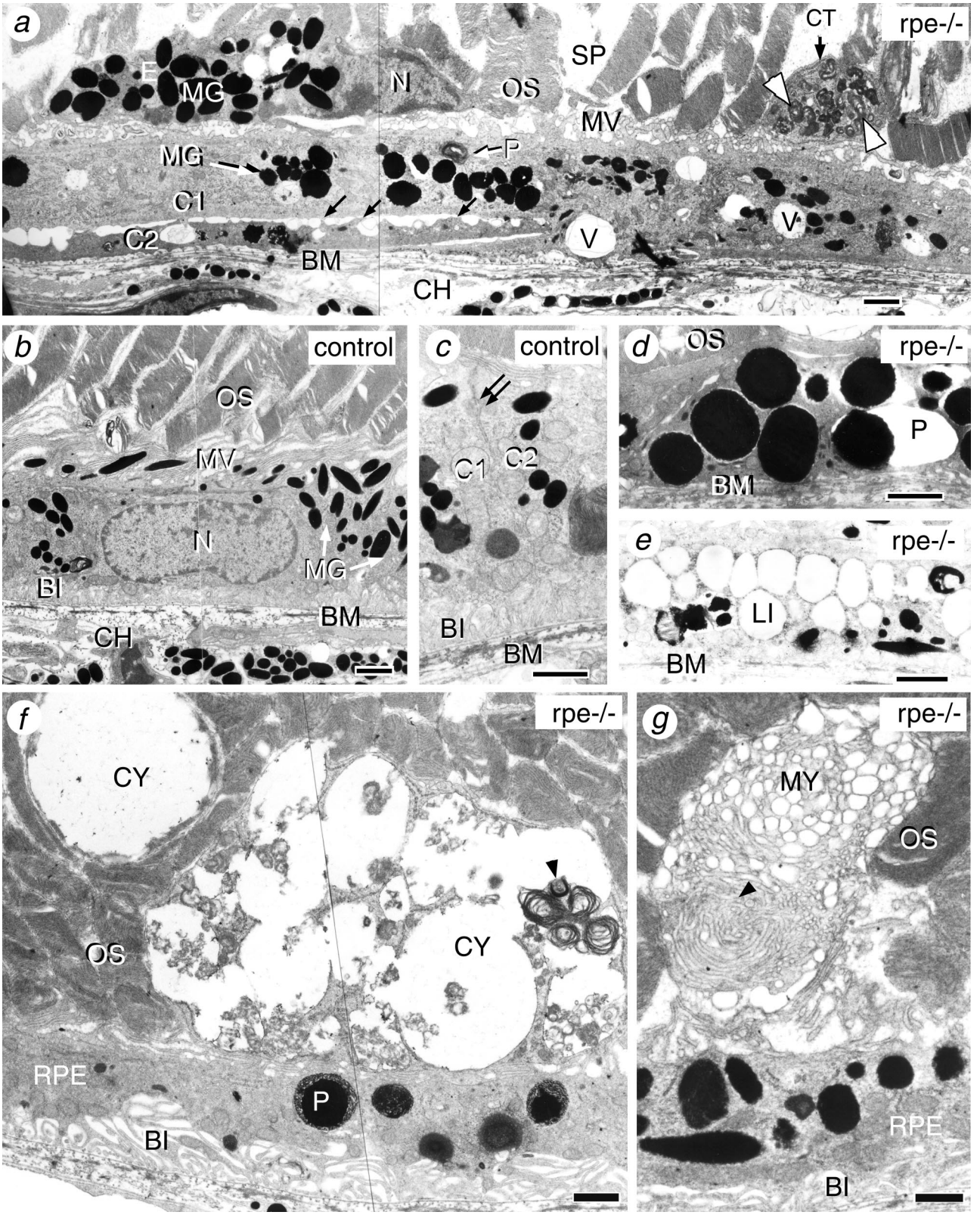

Figure 5. Ultrastructural defects in RPE and photoreceptor cells of 3-month-old RXR$\alpha^{rpe-/-}$ (rpe−/−; **a**, **d**–**g**) and control (**b** and **c**) mice. **Black arrows** in **a** indicate intercellular contact points; the **double arrow** in **d** points to a tight junction. **White** (**a**) and **black** (**f** and **g**) **arrowheads** point to debris of outer segment disks. C1 and C2 in (**a** and **c**) indicate adjacent RPE cells. BI, basal membrane infoldings; BM, Bruch's membrane; CH, choroid; CT, cytoplasmic fragment; CY, cyst; E, ectopic RPE cell; LI, lipid droplet; MG, melanin granules; MV, microvilli; MY, myeloid structure; N, RPE cell nucleus; OS, photoreceptor outer segments; P, phagosome or phagolysosome; SP, intercellular space; V, vacuoles. Scale bar, 1 μm.

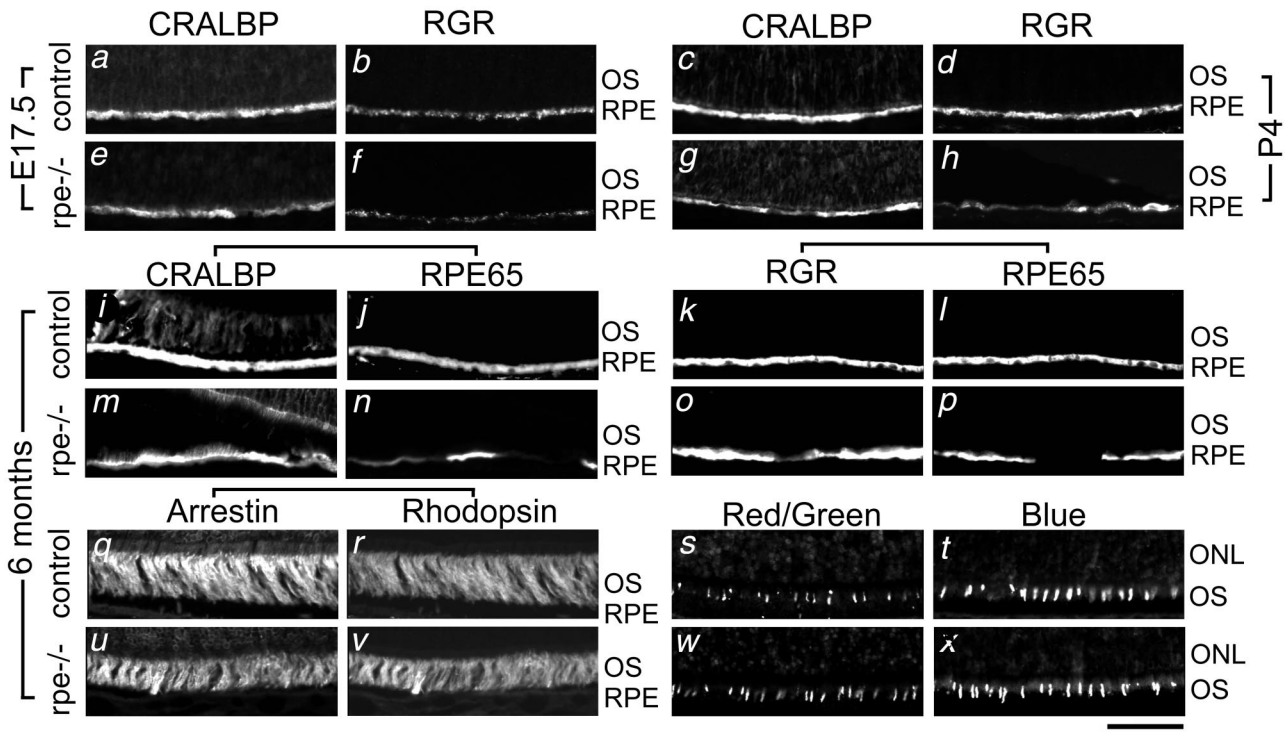

Figure 6. Immunohistochemical analysis of vision-related molecules in RPE and photoreceptor cells of control (**a–d**, **i–l**, **q–t**) and RXRα $^{rpe-/-}$ (rpe−/−; **e–h**, **m–p**, **u–x**) mice. CRALBP and RGR single labelings at E17.5 (**a** and **e** and **b** and **f**, respectively) and P4 (**c** and **g** and **d** and **h**, respectively). Double labeling for CRALBP/RPE65 (**i**, **j**, **m**, and **n**), RGR/RPE65 (**k**, **l**, **o**, and **p**) and arrestin/rhodopsin (**q**, **r**, **u**, and **v**) at 6 months. Cone red/green and blue pigment single labelings at 6 months (**s** and **w** and **t** and **x**, respectively). ONL, outer nuclear layer; OS, outer segment. Scale bar, 50 μm.

nuclear rows in the outer nuclear layer was significantly smaller (83%, 80%, and 78% of controls at 3, 12, and 18 months, respectively; Figure 4, a, b, e, f, and j). Moreover, there was a significant reduction in outer segment lengths and number of nuclear rows in RXRα $^{rpe-/-}$ retinas analyzed at 3, 12, and 18 months when compared with the situation at 1 month (Figure 4, i and j). The severity of these alterations was similar in the center and periphery of the retina (data not shown). No abnormalities were observed in the other cell types of the neural retina (eg, INL; Figure 4, a, b, e, and f). The retinas of RXRα $^{rpe+/-}$ mice at 3, 12, and 18 months did not show any alteration (data not shown).

Electron microscopy analysis revealed the presence of large and irregular intercellular spaces (SP, Figure 5a) between the photoreceptor outer segments. On the apical side of the RPE, cytoplasmic fragments (CT, Figure 5a), large cysts (CY, Figure 5f), and myeloid bodies (MY, Figure 5g) were observed. All these abnormal structures contained altered outer segment disk membranes (Figure 5, a, f, and g; arrowheads). These observations indicate that RXRα $^{rpe-/-}$ mice display, in addition to defects in the RPE, structural alterations in outer segments of photoreceptor cells as well as a progressive loss of these cells.

Distribution in RXRα $^{rpe-/-}$ Eyes of Proteins Involved in Vision

To get insight into the molecular mechanisms underlying the morphological and functional abnormalities of RXRα $^{rpe-/-}$ mice, the expression of three proteins involved in visual retinoid renewal in the RPE, namely, cellular retinaldehyde-binding protein (CRALBP), RPE retinal G-protein-coupled receptor (RGR), and RPE65, were analyzed by immunohistochemistry and semiquantitative RT-PCR in E17.5, P4, P12, and/or 6-month-old mice. The immunostaining patterns for these three proteins were similar at P12 and at 6 months of age (data not shown). CRALBP was detected throughout the RPE in the RXRα $^{rpe-/-}$ and control mice at all ages, but its distribution was less uniform in the mutant RPE (Figure 6; compare a and e, c and g, i and m). RGR labeling was globally decreased in the mutant RPE at E17.5 (Figure 6, compare b and f), and unevenly reduced at P4, P12, and 6 months (Figure 6, compare d and h and k and o, and data not shown). RPE65 was not expressed at E17.5 and P4 (data not shown). RPE65 immunolabeling was weak or absent in some regions of the mutant RPE at 6 months, whereas it was homogeneous in the RPE from control mice (Figure 6, compare j and n and l and p). Importantly, loss of RPE65 labeling was observed in areas where CRALBP or RGR labeling was strong, demonstrating that this loss did not merely reflect a local thinning of the RPE (Figure 6, compare m and n and o and p). In agreement with these results, semiquantitative RT-PCR analyses of 6-month-old eyecups revealed an ~50% reduction of RPE65, CRALBP, and RGR transcripts (Figure 7). In 6-month-old mice, the expression patterns of photoreceptor markers (rhodopsin, arrestin, blue and red/green cone pigments) were also analyzed. The distributions of arrestin and rhodopsin, as well as those of cone blue pigment in the

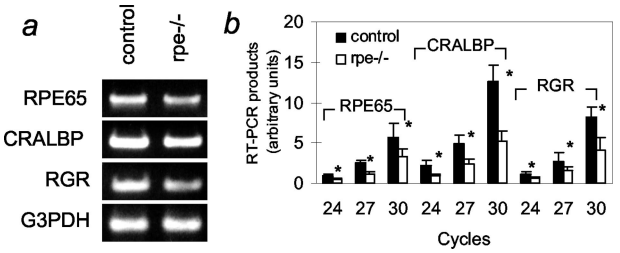

Figure 7. Vision-related gene transcript levels in RPE of RXR$\alpha^{rpe-/-}$ mice. Total RNA from 6-month-old control and RXR$\alpha^{rpe-/-}$ eye cups was analyzed by RT-PCR for RPE65, CRALBP, and RGR. G3PHD was used as an invariant internal control. **a:** Products after 30 (RPE65, CRALBP, and RGR) and 21 (G3PDH) cycles. **b:** Quantification of the RT-PCR products for RPE65, CRALBP, and RGR. Mean ± SD ($n = 3$); *, $P < 0.01$.

inferior hemisphere and of red/green cone pigment in the superior hemisphere (where they are normally concentrated) were similar in RXR$\alpha^{rpe-/-}$ and control mice (Figure 6, compare q to t and u to x).

Absence of TUNEL-Positive Cells in RXR$\alpha^{rpe-/-}$ Eyes

Apoptotic cells were undetectable in sections from both RXR$\alpha^{rpe-/-}$ and control eyes, although all cell nuclei were positive in DNase I-treated histological sections, which served as positive controls in these assays (data not shown).

Discussion

We show here that selective ablation of RXRα in RPE cells causes morphological defects and reduced expression in RPE cells of proteins involved in visual retinoid renewal. Moreover, the morphological and functional alterations occurring in the neural retina under these conditions most probably arise as a consequence of RPE defects.

RPE Cell Functions Require RXRa

In RXR$\alpha^{rpe-/-}$ mice, excision of the RXRα gene, which is observed in more than 95% of adult RPE cells, is already detected throughout the RPE at E13.5[22] and the RXRα protein is efficiently removed from the RPE at this stage (present results). The altered expression of RGR and CRALBP in the RPE of RXR$\alpha^{rpe-/-}$ mice is observed at E17.5, indicating early functions of RXRα in these cells. However, there is a lag between the time window at which RXRα is highly expressed in the wild-type RPE, ie, E10.5 to E17.5,[28] and the onset of the morphological defects in the RPE of RXR$\alpha^{rpe-/-}$ mice, ie, P12. Along the same lines, it is noteworthy that histological defects were not observed in the RPE of RXRα-null mutant mice that die before E16.5.[4] Thus, the lack of RXRα in prenatal RPE apparently impairs cellular functions that are normally required for late postnatal steps in the maturation of RPE cells.

The RPE cells of adult RXR$\alpha^{rpe-/-}$ mice display several defects. They are very flat, overlap primarily with their neighbors, and are occasionally ectopically located between photoreceptor outer segments. They possess poorly developed apical microvilli and basal membrane infoldings as well as fewer phagosomes. They also show abnormal organelles such as large phagolysosomes and vacuoles, as well as numerous lipid droplets. Paucity of RPE phagosomes as well as flattening, overlapping, and migration of RPE cells are characteristics of Royal College Surgeons (RCS) rats that display a retinal degeneration related to a defective phagocytosis by RPE cells of outer segment disks.[29,30] The decrease in phagosome numbers might be even larger at peak time of phagocytosis, ie, ~1 hour after the onset of light as in the case of RCS rats.[31] It is thus probable that phagocytosis of outer segment disks is defective in RXR$\alpha^{rpe-/-}$ mice. Lipid droplets are abundant in the RPE of null mutants for RPE65,[13] and *all-trans*-retinyl esters accumulate in eyes of mice carrying null mutations for RPE65,[13] CRALBP,[17] or RGR.[15] As RXR$\alpha^{rpe-/-}$ mice show altered expression of CRALBP, RGR and RPE65, the presence of lipid droplets in their RPE cells may result from accumulation of visual retinoids. Absence of detectable atrophy of choroid structures in RXR$\alpha^{rpe-/-}$ mice by transmission electron microscopy suggests that the defects of the RPE cells are milder than those caused by pharmacological and surgical means that are associated with choriocapillaris degeneration.[32,33] However, more detailed analysis, eg, scanning electron microscopy of choroidal vascular casts, may reveal more subtle RPE-related changes in the choriocapillaris, as in the case of senescence-accelerated mice.[34]

Photoreceptor Cell Abnormalities and Functional Alterations of Photoreceptor-RPE Complex Arising from RPE Defects

The reduction of ERG responses by ~50% in RXR$\alpha^{rpe-/-}$ mice may be accounted for by a decrease in available opsin molecules resulting from the shortening of photoreceptor outer segments. Because expressions of RGR, RPE65, and CRALBP, which are normally required for regeneration of *11-cis*-retinaldehyde in the RPE,[13,15,17] are decreased in the mutant RPE, the delayed dark adaptation after photo bleach may be secondary to a reduced supply of *11-cis*-retinaldehyde to opsins. The reductions of both scotopic and photopic ERG responses suggest that both rod and cone pathways are affected by ablation of RXRα in the RPE.

The presence in RXR$\alpha^{rpe-/-}$ mice of large cysts and myeloid bodies that contain outer segment debris among photoreceptor outer segments and the decrease in the number of RPE phagosomes suggest that processing of shed outer segments by RPE cells is not fully efficient. The disorganization of photoreceptor cell outer segments, as well as the decrease of photoreceptor cell number may result from deficient processing of shed outer segment disks as in the case of RCS rats,[29,30] or alternatively, from impaired visual transduction in the photoreceptors as in the case of RPE65-null mice.[13] Absence of apoptotic cells in RXR$\alpha^{rpe-/-}$ eyes suggests

mild dystrophy of the photoreceptors, which is compatible with the survival of 78% of these cells in 18-month-old mutant mice. It is noteworthy recalling that, in our mutant mice, the floxed RXRα gene is not only excised throughout the RPE, but also in limited populations of the neural retina cells representing, in adults, less than 5% of the cells in the center and less than 30% in the periphery.[22] However, as the severity of outer segment abnormalities is not different between the periphery and center of the RXRα $^{rpe-/-}$ retina, it is unlikely (although not definitely ruled out) that they result from RXRα ablation in the neural retina.

Which Signaling Pathways Are Altered in RXRα $^{rpe-/-}$ Mice?

Nuclear receptors expressed in RPE cells which could act as RXRα heterodimeric partners for RPE homeostasis include retinoic acid receptor (RAR) α, β, and γ; peroxisome proliferator-activated receptors (PPAR) α, β, and γ; NGFI-B; and RNR.[26,28,35–37] Interestingly, mutant mice lacking both RARβ2 and RARγ2 isoforms (RARβ2/RARγ2 double-null mutants) show defects that are similar to those observed in RXRα $^{rpe-/-}$ mice, including flattening and vacuolation of RPE cells as well as disorganization of photoreceptor outer segments,[26] although they start earlier and are, on the whole, more severe than those seen in RXRα $^{rpe-/-}$ mice. There is strong evidence, from gene knockout studies, for the existence of functional RXRα/RAR(β and γ) heterodimers *in vivo*.[4,38,39] Altogether, these data raise the possibility that RXRα/RARβ2 and RXRα/RARγ2 heterodimers could transduce a retinoid signal required for the RPE homeostasis. On the other hand, accumulation of lipids in RPE cells was not observed in RARβ2/RARγ2 double-null mutants supporting the view that signaling pathways other than those mediated by RXRα/RAR heterodimers may be affected in RXRα $^{rpe-/-}$ mice. Note that the relatively late onset and slow progression of the phenotype, as well as the heterogeneity of expression levels of RPE65, CRALBP, or RGR in the RPE of the RXRα $^{rpe-/-}$ mice may result from a partial functional compensation of the loss of RXRα by RXRβ that is also expressed in the developing and adult RPE.[28]

CRALBP- and RGR-null mutants show delayed dark adaptation, but no morphological abnormalities in the RPE and photoreceptor cells.[15,17] RPE65-null mutants exhibit delayed dark adaptation and disorganized photoreceptor outer segments with a small decrease in the number of photoreceptor cells, but no morphological alterations in the RPE except for lipid droplets.[13] Thus, CRALBP, RGR, and RPE65 represent most probably only a fraction of the altered protein profile in RXRα $^{rpe-/-}$ mice. Interestingly, RNR can interact with the promoter of the CRALBP gene in the presence of RXR,[37] thus raising the possibility that the alteration of CRALBP in the RXRα $^{rpe-/-}$ mice may result from a loss of transcriptional regulation by RXRα/RNR heterodimers.

Relevance to Human Retinal Diseases

The phenotype of the RXRα $^{rpe-/-}$ mice does not correspond accurately to any of known human retinal disease. For instance, it differs markedly from retinitis pigmentosa and its allied diseases, in which rod photoreceptors are primarily affected and almost completely lost.[40] Instead, this abnormal mouse phenotype is more reminiscent of diseases that primarily involve the RPE. Such diseases may include age-related macular degeneration.[18,19] RXRα $^{rpe-/-}$ mice show some phenotypic features similar to those of age-related macular degeneration patients, ie, thinning and depigmentation of RPE cells and modest loss of photoreceptor cells, but do not display the sub-RPE deposit that is a hallmark of this disease.[41] Nevertheless, our mice should provide a useful model for studying RXRα signaling pathways in the RPE which may be involved in pathogenesis and may represent potential therapeutic targets of human retinal diseases.

Acknowledgments

We thank Dr. Debra Thompson for the RPE65 antibody, Dr. Henry Fong for the RGR antibody, Dr. John Saari for the CRALBP antibody, Dr. David Hicks for the rhodopsin antibody, Dr. Yvonne de Kozak for the arrestin antibody, Dr. Jeremy Nathans for the cone blue and red/green pigment antibodies, Dr. Norbert Ghyselinck for helpful discussion, and Bruno Weber and Noelle Hanoteau for technical assistance.

References

1. Hyatt GA, Dowling JE: Retinoic acid. A key molecule for eye and photoreceptor development. Invest Ophthalmol Vis Sci 1997, 38: 1471–1475
2. Drager U, McCaffery P: Retinoic acid and development of the retina. Prog Retin Eye Res 1997, 16:323–351
3. Chambon P: The retinoid signaling pathway: molecular and genetic analyses. Semin Cell Biol 1994, 5:115–125
4. Kastner P, Grondona JM, Mark M, Gansmuller A, LeMeur M, Decimo D, Vonesch JL, Dolle P, Chambon P: Genetic analysis of RXRα developmental function: convergence of RXR and RAR signaling pathways in heart and eye morphogenesis. Cell 1994, 78:987–1003
5. Saari J: Biochemistry of visual pigment regeneration. Invest Ophthalmol Vis Sci 2000, 41:337–348
6. McBee J, Palczewski K, Baehr W, Pepperberg D: Confronting complexity: the interlink of phototransduction and retinoid metabolism in the vertebrate retina. Prog Retin Eye Res 2001, 20:469–529
7. Bok D: The retinal pigment epithelium: a versatile partner in vision. J Cell Sci 1993, 17:189–195
8. Nguyen-Legros J, Hicks D: Renewal of photoreceptor outer segments and their phagocytosis by the retinal pigment epithelium. Int Rev Cytol 2000, 196:245–313
9. Raymond SM, Jackson IJ: The retinal pigmented epithelium is required for development and maintenance of the mouse neural retina. Curr Biol 1995, 5:1286–1295
10. Gu S, Thompson D, Srikumari C, Lorenz B, Finckh U, Nicoletti A, Murthy K, Rathmann M, Kumaramanickavel G, Denton M, Gal A: Mutations in RPE65 cause autosomal recessive childhood-onset severe retinal dystrophy. Nat Genet 1997, 17:194–197
11. Marlhens F, Bareil C, Griffoin J, Zrenner E, Amalric P, Eliaou C, Liu S, Harris E, Redmond T, Arnaud B, Claustres M, Hamel C: Mutations in RPE65 cause Leber's congenital amaurosis. Nat Genet 1997, 17: 139–141

12. Morimura H, Fishman G, Grover S, Fulton A, Berson E, Dryja T: Mutations in the RPE65 gene in patients with autosomal recessive retinitis pigmentosa or Leber congenital amaurosis. Proc Natl Acad Sci USA 1998, 95:3088–3093
13. Redmond T, Yu S, Lee E, Bok D, Hamasaki D, Chen N, Goletz P, Ma J, Crouch R, Pfeifer K: Rpe65 is necessary for production of 11-cis-vitamin A in the retinal visual cycle. Nat Genet 1998, 20:344–351
14. Morimura H, Saindelle-Ribeaudeau F, Berson E, Dryja T: Mutation in RGR, encoding a light-sensitive opsin homologue, in patients with retinitis pigmentosa. Nat Genet 1999, 23:393–394
15. Chen P, Hao W, Rife L, Wang X, Shen D, Chen J, Ogden T, Van Boemel G, Wu L, Yang M, Fong H: A photic visual cycle of rhodopsin regeneration is dependent on Rgr. Nat Genet 2001, 28:256–260
16. Maw M, Kennedy B, Knight A, Bridges R, Roth K, Mani E, Mukkadan J, Nancarow D, Crabb J, Denton M: Mutation of the gene encoding cellular retinaldehyde-binding protein in autosomal recessive retinitis pigmentosa. Nat Genet 1997, 17:198–200
17. Saari J, Nawrot M, Kennedy B, Garwin G, Hurley J, Huang J, Possin D, Crabb J: Visual cycle impairment in cellular retinaldehyde binding protein (CRALBP) knockout mice results in delayed dark adaptation. Neuron 2001, 29:739–748
18. Fine S, Berger J, Maguire M, Ho A: Age-related macular degeneration. N Engl J Med 2000, 342:483–492
19. Bok D: New insights and new approaches toward the study of age-related macular degeneration. Proc Natl Acad Sci USA 2002, 99: 14619–14621
20. Beermann F: The tyrosinase related protein-1 (Tyrp1) promoter in transgenic experiments: targeted expression to the retinal pigment epithelium. Cell Mol Biol 1999, 45:961–968
21. Metzger D, Chambon P: Site- and time-specific gene targeting in the mouse. Methods 2001, 1:71–80
22. Mori M, Metzger D, Garnier G-M, Chambon P, Mark M: Site-specific somatic mutagenesis in the retinal pigment epithelium. Invest Ophthalmol Vis Sci 2002, 43:1384–1388
23. Li M, Chiba H, Warot X, Messaddeq N, Gerard C, Chambon P, Metzger D: RXRα ablation in skin keratinocytes results in alopecia and epidermal alterations. Development 2001, 128:675–688
24. Pittler S, Baehr W: Identification of a nonsense mutation in the rod photoreceptor cGMP phosphodiesterase beta-subunit gene of the rd mouse. Proc Natl Acad Sci USA 1991, 88:8322–8326
25. Taketo M, Schroeder A, Mobraaten L, Gunning K, Hanten G, Fox R, Roderick T, Stewart C, Lilly F, Hansen C, Overbeek P: FVB/N: an inbred mouse strain preferable for transgenic analyses. Proc Natl Acad Sci USA 1991, 88:2065–2069
26. Grondona J, Kastner P, Gansmuller A, Decimo D, Chambon P, Mark M: Retinal dysplasia and degeneration in RARβ2/RARγ2 compound mutant mice. Development 1996, 122:2173–2188
27. Duncan J, LaVail M, Yasumura D, Matthes M, Yang H, Trautmann N, Chappelow A, Feng W, Earp H, Matsushima G, Vollrath D: An RCS-like retinal dystrophy phenotype in mer knockout mice. Invest Ophthalmol Vis Sci 2003, 44:826–838
28. Mori M, Ghyselinck N, Chambon P, Mark M: Systemic immunolocalization of retinoid receptors in developing and adult mouse eyes. Invest Ophthalmol Vis Sci 2001:1312–1318
29. Dowling J, Sideman R: Inherited retinal dystrophy in the rat. J Cell Biol 1962, 14:73–109
30. LaVail M: Legacy of the RCS rat: impact of a seminal study on cell biology and retinal degenerative diseases. Prog Brain Res 2001, 131:617–627
31. Goldman A, O'Brien P: Phagocytosis in the retinal pigment epithelium of the RCS rat. Science 1978, 201:1023–1025
32. Korte G, Reppucci V, Henkind P: RPE destruction causes choriocapillary atrophy. Invest Ophthalmol Vis Sci 1984, 25:1135–1145
33. Del Priore L, Hornbeck R, Kaplan H, Jones Z, Valentino T, Mosinger-Ogilvie J, Swinn M: Debridement of the pig retinal pigment epithelium in vivo. Arch Ophthalmol 1995, 113:939–944
34. Majji A, Cao J, Chang K, Hayashi A, Aggarwal S, Grebe R, De Juan EJ: Age-related retinal pigment epithelium and Bruch's membrane degeneration in senescence-accelerated mouse. Invest Ophthalmol Vis Sci 2000, 41:3936–3942
35. Ershov A, Lukiw W, Bazan N: Selective transcription factor induction in retinal pigment epithelial cells during photoreceptor phagocytosis. J Biol Chem 1996, 271:28458–28462
36. Elshov A, Bazan G: Photoreceptor phagocytosis selectively activates PPARgamma expression in retinal pigment epithelial cells. J Neurosci Res 2000, 60:328–337
37. Chen F, Figueroa D, Marmorstein A, Zhang Q, Petrukhin K, Caskey C, Austin C: Retina-specific nuclear receptor: a potential regulator of cellular retinaldehyde-binding protein expressed in retinal pigment epithelium and Muller glial cells. Proc Natl Acad Sci USA 1999, 96:15149–15154
38. Mascrez B, Mark M, Dierich A, Ghyselinck N, Kastner P, Chambon P: The RXRalpha ligand-dependent activation function 2 (AF-2) is important. Development 1998, 125:4691–4707
39. Mascrez B, Mark M, Krezel W, Dupe V, LeMeur M, Ghyselinck N, Chambon P: Differential contributions of AF-1 and AF-2 activities to the developmental functions of RXR alpha. Development 2001, 128: 2049–2062
40. Weleber R, Gregory-Evans K: Retinitis pigmentosa and allied disorders. Retina. Edited by S Ryan. St. Louis, Mosby, 2001, pp 362–470
41. Green W: Histopathology of age-related macular degeneration. Mol Vis 1999, 5:27–37